

## BOSE-EINSTEIN CONDENSATES ON A PERMANENT MAGNETIC FILM ATOM CHIP

B. V. HALL, S. WHITLOCK, F. SCHARNBERG\*  
P. HANNAFORD AND A. SIDOROV

*ARC Centre of Excellence for Quantum-Atom Optics and  
Centre for Atom Optics and Ultrafast Spectroscopy  
Swinburne University of Technology, Melbourne, Victoria 3122, Australia  
E-mail: brhall@swin.edu.au*

We present a permanent magnetic film atom chip based on perpendicularly magnetized TbGdFeCo films. This chip routinely produces a Bose-Einstein condensate (BEC) of  $10^5$   $^{87}\text{Rb}$  atoms using the magnetic film potential. Fragmentation observed near the film surface provides unique opportunities to study BEC in a disordered potential. We show this potential can be used to simultaneously produce multiple spatially separated condensates. We exploit part of this potential to realize a time-dependent double well system for splitting a condensate.

### 1. Introduction

A recent advance in the field of quantum degenerate gases has been the development of the atom chip<sup>1,2,3</sup>. This device streamlines BEC production by exploiting tightly confining atom traps realized near a micro-structured magnetic field source<sup>4</sup>. Additionally these sources can be tailored for the manipulation of coherent matter waves and recently used to demonstrate interference of a BEC in a double well potential<sup>5,6</sup>. Several technical limitations have been identified for atom chips where micro-structured current-carrying wires provide magnetic confinement<sup>7</sup>. Current noise can cause spin flip loss in addition to in-trap heating. Methods of conductor fabrication also impose limitations as wire edge roughness induces fragmentation of ultracold atom clouds<sup>8</sup>. Moreover a fundamental spin-flip loss mechanism caused by thermally induced current fluctuations is inherently large in conducting materials<sup>9</sup>. Some of these limitations can be addressed though

---

\*Present address: Institut für Quantenoptik, Universität Hannover, 30167 Hannover, Germany

the implementation of atom chips which use permanent magnetic materials as configurable magnetic field sources<sup>10,11</sup>. Permanent magnetic materials have intrinsically low magnetic field noise, exhibit reduced spin-flip loss rates and allow tighter confinement close to the magnet surface<sup>12,13</sup>.

In this paper we report on recent experiments performed with an atom chip that incorporates a perpendicularly magnetized, permanent magnetic film.

## 2. Atom chip: design and construction

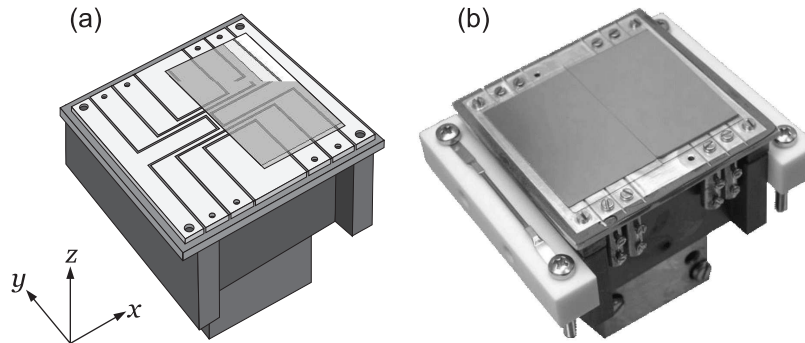


Figure 1. A schematic (a) and an image (b) of the atom chip. From the top down: two adjacent gold coated glass slides (1×TbGdFeCo, 1×blank), machined Ag foil H-shape wire with end wires, Shapal-M base-plate and Cu heat sink.

A schematic diagram and photographic image of the permanent magnetic film atom chip is shown in Fig. 1. The atom chip is based upon a single rectangular slab of uniformly magnetized TbGdFeCo film with a thickness  $h$ . The film is mounted in the  $xy$  plane, with one long edge parallel to the  $y$  axis. The magnetic field produced by this slab is the same as that from an equivalent current ( $I_{eff} = hM_R$ ) that propagates around the slab perimeter<sup>14</sup>. The magnitude of the field near this edge is given by

$$B_{film} = \frac{\mu_0}{2\pi} \frac{hM_R}{z}, \quad (1)$$

where  $z$  is the distance from the film. A uniform field  $B_x$  cancels the film field at a height  $z_0$ , resulting in a two-dimensional quadrupole potential which can be used as an atomic waveguide for weak-field seeking atoms. A three-dimensional (3D) magnetic trap is achieved by pinching off this guide

with a nonuniform axial field  $B_y$ . This field is made by two parallel current-carrying end wires, located beneath and perpendicular to the waveguide. A nonzero  $B_y$  suppresses Majorana spin-flip loss while creating a harmonic potential with a radial frequency

$$2\pi f_{rad} = \frac{\mu_0}{2\pi} \frac{hM_R}{z_0^2} \sqrt{\frac{\mu_B g_F m_F}{m B_y}}, \quad (2)$$

where  $\mu_B g_F m_F$  is the usual Zeeman factor and  $m$  is the atomic mass.

The top layer of the atom chip consists of two adjacent  $40 \times 23 \times 0.3 \text{ mm}^3$  glass slides. One slide has a uniformly magnetized TbGdFeCo coating and both have a reflective gold overlayer. The large reflective area is beneficial for efficiently collecting atoms in a reflection magneto-optical trap (MOT) near the surface within a single UHV system. A multilayered deposition technique was used to produce the film with a composition of  $\text{Tb}_6\text{Gd}_{9.6}\text{Fe}_{80}\text{Co}_{4.4}$ . This material has properties advantageous to integrated atom optics, including large perpendicular anisotropy, high Curie temperature ( $T_C = 300 \text{ }^\circ\text{C}$ ), large coercivity ( $H_C$ ), strong remanent magnetization ( $M_R$ ) and excellent magnetic homogeneity. A detailed account of the TbGdFeCo films and the atom chip will be reported elsewhere<sup>15</sup>. The film used on the chip has a remanent magnetization of  $\mu_0 M_R = 0.28 \text{ T}$  for a total magnet thickness of  $900 \text{ nm}$  ( $hM_R = 0.20 \pm 0.01 \text{ A}$ ). A tight trap of frequency  $f_{rad} \approx 1 \text{ kHz}$  is obtained approximately  $70 \text{ }\mu\text{m}$  above the film using modest values of  $B_x = 0.56 \text{ mT}$  and  $B_y = 0.1 \text{ mT}$ . While this trap is excellent for evaporative cooling, it has neither the depth nor the spatial extent to be loaded directly by a MOT.

To provide large, time-dependent potentials, a machined silver foil structure was designed to sit beneath the magnetic film<sup>16</sup>. The foil is  $0.5 \text{ mm}$  thick and machined in an H-shape with additional end wires either side (Fig. 1a). The foil is epoxied to a Shapal-M ceramic plate and  $500 \text{ }\mu\text{m}$  insulating grooves were cut with a computer controlled PCB mill. The conductor cross section is  $1.0 \times 0.5 \text{ mm}^2$  facilitating the use of high currents ( $> 30 \text{ A}$ ). The H-shape structure allows rapid switching between a U-shape ( $I_U$ ) or Z-shape ( $I_Z$ ) current path. This provides a 3D quadrupole field geometry to form a U-wire MOT or an Ioffe-Pritchard ( $IP$ ) magnetic potential, respectively<sup>17</sup>. The two glass slides, silver foil structure and ceramic plate are screwed to a copper heat sink with two rubidium dispensers and is mounted upside down in the vacuum chamber.

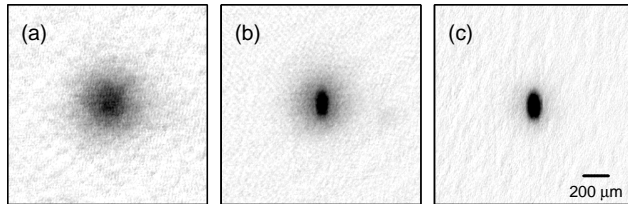


Figure 2. Absorption images of an atom cloud after 30 ms of ballistic expansion from a permanent magnetic film trap. Images correspond to (a) a thermal cloud, (b) a partially condensed cloud and (c) an almost pure condensate.

### 3. BEC on the permanent magnetic film

A reflection MOT is loaded via a pulsed Rb dispenser where  $2 \times 10^8$  atoms are collected 4.6 mm from the surface. After 15 s hold time the atoms are transferred and compressed into a U-wire MOT located 1.6 mm from the film surface. After short polarization gradient cooling and optical pumping stages  $4 \times 10^7$  atoms are transferred into the Z-wire *IP* trap. Atoms are then moved to  $560 \mu\text{m}$  from the surface where the radial trap frequency is  $2\pi \times 530 \text{ Hz}$  and the elastic collision rate is high enough to begin forced evaporative cooling. Evaporation to the BEC transition is a two step process. For the first 8.85 s of a single 10 s logarithmic radio frequency (RF) sweep, atoms are cooled to a temperature of  $\sim 5 \mu\text{K}$ . Then the RF amplitude is reduced to zero for 150 ms while the atoms are transferred to the magnetic film trap at  $z = 90 \mu\text{m}$  ( $f_{rad} = 700 \text{ Hz}$ ,  $f_{ax} = 8 \text{ Hz}$ ,  $I_Z = 0 \text{ A}$  and  $I_{end} = 6 \text{ A}$ ). An additional uniform magnetic field tunes the trap bottom to minimize any discontinuity in the evaporation trajectory. Finally the RF amplitude is increased and evaporation continues for 1 s to the BEC phase transition. Before imaging, the magnetic film trap is moved  $170 \mu\text{m}$  from the surface. Both  $I_{end}$  and  $B_x$  are rapidly turned off, leaving the atoms to ballistically expand with minor acceleration from the permanent field gradient. Figure 2 shows absorption images of a ballistically expanded cloud of atoms crossing the BEC phase transition. The apparatus creates a new condensate of  $1 \times 10^5$  atoms in the magnetic film trap every 50 s.

### 4. Characterization of the magnetic film potential

An *in situ* measurement of the film magnetization allows the BEC to be used as a highly sensitive magnetic field probe. The small spatial extent of the BEC allows accurate position information to be obtained by absorption imaging. Since the BEC is localized at the magnetic field minimum (where

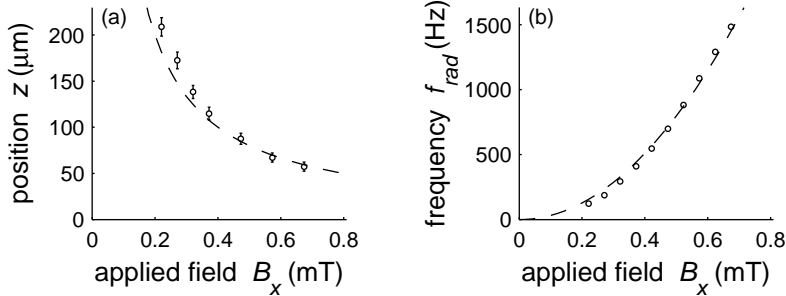


Figure 3. Measurements of the trap position from the film surface (a) and of the trap frequency (b) as a function of applied field  $B_x$ . The data (open circles) agrees well with predictions (dashed line) of equations 1 and 2. The discrepancy of position for low fields can be accounted for by including the effect of gravity.

$B_{film} = -B_x$ ) a measure of distance from the film versus  $B_x$  yields  $\hbar M_R$ . The narrow momentum distribution of a BEC also allows excellent resolution when performing RF spectroscopy on the trapped atoms. A short RF pulse provides an absolute measurement of  $B_x$  by observing the resonant population of the  $F = 2, m_F = -2, -1, 0, 1, 2$  states. Each magnetic state of a freely falling cloud is spatially separated by a field gradient provided by  $I_Z$ . The magnetic potential is further characterized by observing centre of mass oscillations. A magnetically trapped condensate is analogous to a high Q resonator since the trap frequency is much higher than the damping rate<sup>18</sup>. By exciting radial centre of mass motion  $f_{rad}$  can be measured to better than 1 Hz. The trap position and the trap frequency have been measured against  $B_x$  and are shown in Fig 3. The data are consistent with the predictions of equations 1 and 2.

In addition to the expected magnetic field from the film we observe a small spatially alternating component of magnetic field parallel to the film edge,  $\Delta B_y$ . This oscillating magnetic field leads to fragmentation of cold clouds near the film surface and can be compared to fragmentation observed near microfabricated wires<sup>8</sup>. Initial observations suggest that  $\Delta B_y$  has an RMS amplitude of  $\sim 4.7 \mu\text{T}$ , 90  $\mu\text{m}$  from the film surface. It appears roughly periodic with a period of 450  $\mu\text{m}$ , however finer structure exists closer to the surface. The relative amplitude of the fragmenting field  $\Delta B_y / \Delta B_{film} \sim 10^{-2}$  is two orders of magnitude larger than that observed above wire based atom chips.

## 5. A string of BECs in a disordered potential

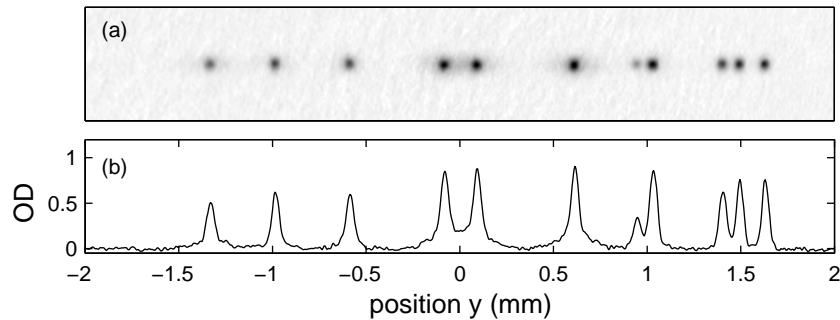


Figure 4. Absorption image (a) and associated optical density profile (b) for multiple condensates realized in the disordered potential. Images are taken after 15 ms of ballistic expansion.

Although the fragmented potential limits the ability to form a smooth atomic waveguide, the micro-structure provides a unique possibility for studying BEC in a disordered potential (Fig. 4). After the initial stages of RF cooling, the thermal cloud is transferred to the magnetic film and allowed to expand axially under weak confinement ( $f_{ax} \approx 1$  Hz). The elongated cloud spans most of the image area ( $\sim 5$  mm). The cloud is then radially compressed and moved closer to the surface where fragmentation becomes significant. An additional 4 s of evaporative cooling is applied using a second RF source. The BEC transition is reached simultaneously across 11 independent potential wells spanning 3 mm. The total number of condensed atoms is comparable to that observed for a single BEC ( $N_{BEC} \sim 1 \times 10^5$ ). The large separation between individual condensates permits addressability by optical means or by RF coupling in a field gradient.

## 6. A double well system for splitting a BEC

The disordered potential produced by the film is rich in structure. It is possible to transport atoms to particular regions along the film in order to perform various experiments. A roughly symmetric double well potential is present near the centre of Fig. 4. A single BEC is formed  $170 \mu\text{m}$  from the surface where the fragmentation is small compared to the chemical potential. By increasing  $B_x$  the condensate moves closer to the surface and begins

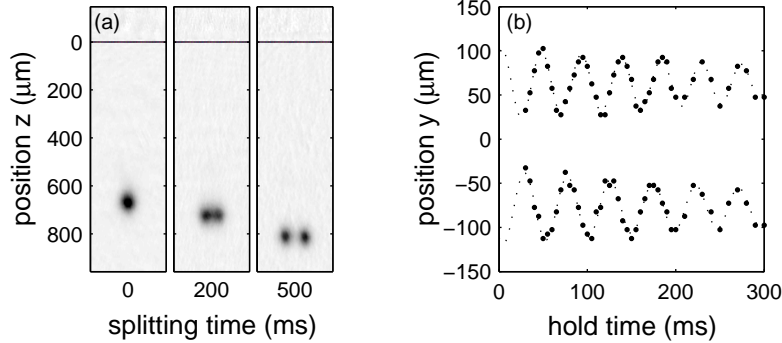


Figure 5. Absorption images (a) of condensates during time dependent splitting in the double well potential. Images were taken after 2 ms of ballistic expansion. The relative position of each cloud is inverted due to additional acceleration from the permanent magnetic field gradient. Axial trap frequencies in the double well (b) were determined by observing centre of mass oscillations.

to separate into two parts (Fig. 5a). To split the condensate evenly, the asymmetry between the two split wells was tuned with a magnetic field gradient to less than 100 nT. The BEC is separated by  $\sim 140 \mu\text{m}$  over 500 ms to avoid unwanted excitations. Shorter splitting times (down to 30 ms) are possible; however out of phase centre of mass oscillations are observed (Fig. 4b). The level of symmetry between the individual trap frequencies is remarkable ( $f_{L,rad} = 281 \text{ Hz}$ ,  $f_{R,rad} = 283 \text{ Hz}$ ,  $f_{L,ax} = 21 \text{ Hz}$ ,  $f_{R,ax} = 22 \text{ Hz}$ ). Unfortunately, the resolution of our imaging system does not permit the observation of interference fringes that would be present in ballistic expansion. Other regions of the potential with smaller features may provide conditions more favourable for investigating coherent splitting and interference of BEC in a double well system.

## 7. Conclusion

We have produced an atom chip that exploits a thick perpendicularly magnetized TbGdFeCo film for the production and manipulation of a BEC. We have used the BEC as a sensitive probe to directly measure the magnetic field associated with the magnetic film. We have shown that this potential is rich in structure and can be exploited for the simultaneous production of multiple condensates. Moreover we have used a part of this potential to demonstrate a controllable double well system that permits the symmetric splitting of a condensate without excitations or excessive heating.

## Acknowledgments

We thank J. Wang and D. Gough for carrying out the magnetic film deposition. This project is supported by the ARC Centre of Excellence for Quantum-Atom Optics and a Swinburne University Strategic Initiative grant.

## References

1. W. Hänsel, P. Hommelhoff, T. W. Hänsch, and J. Reichel, *Nature* **413**, 498 (2001).
2. H. Ott, J. Fortágh, A. Grossmann and C. Zimmermann, *Phys. Rev. Lett.* **87**, 230401 (2001).
3. R. Folman, P. Krueger, J. Schmiedmayer, J. Denschlag and C. Henkel, *Adv. At. Mol. Opt. Phys.* **48**, 236 (2002).
4. S. Du, M. B. Squires, Y. Imai, L. Czaia, R. A. Saravanan, V. Bright, J. Reichel, T. W. Hänsch and D. Anderson, *Phys. Rev. A* **70**, 053606 (2004).
5. Y. Shin, C. Sanner, G. B. Jo, T. A. Pasquini, M. Saba, W. Ketterle and D. E. Pritchard, *arXiv:cond-mat/0506464* (2005).
6. T. Schumm, S. Hofferberth, L. M. Andersson, S. Wildermuth, S. Groth, I. Bar-Joseph, J. Schmiedmayer and P. Krüger, *arXiv:quant-ph/0507047* (2005).
7. C. Henkel, P. Krüger, R. Folman and J. Schmiedmayer, *Appl. Phys. B* **76**, 173182 (2003).
8. J. Estève, C. Aussibal, T. Schumm, C. Figl, D. Mailly, I. Bouchoule, C. I. Westbrook and A. Aspect, *Phys. Rev. A* **70**, 043629 (2004).
9. M. P. A. Jones, C. J. Vale, D. Sahagun, B. V. Hall and E. A. Hinds, *Phys. Rev. Lett.* **91**, 080401 (2003).
10. E. A. Hinds and I. G. Hughes, *J. Phys. D: App. Phys.* **32**, R119 (1999).
11. S. Eriksson, F. Ramirez-Martinez, E. A. Curtis, B. E. Sauer, P. W. Nutter, E. W. Hill and E. A. Hinds, *Appl. Phys. B* **79**, 811 (2004).
12. C. D. J. Sinclair, E. A. Curtis, I. Llorente Garcia, J. A. Retter, B. V. Hall, S. Eriksson, B. E. Sauer and E. A. Hinds, *Eur. Phys. J. D* **35**, 105-110 (2005).
13. S. Scheel, P. K. Rekdal, P. L. Knight and E. A. Hinds, *arXiv:quant-ph/0501149*(2005).
14. J. D. Jackson, *Classical Electrodynamics* 3rd (1999) edition (New York: Wiley) chap 5.
15. B. V. Hall, S. Whitlock, F. Scharnberg, P. Hannaford and A. Sidorov, *arXiv:quant-ph/0507435* (2005).
16. C. J. Vale, B. Ucroft, M. J. Davis, N. R. Heckenberg and H. Rubinsztein Dunlop, *J. Phys. B: At. Mol. Opt. Phys.* **37**, 29592967 (2004).
17. J. Reichel, W. Hänsel and T. W. Hänsch, *Phys. Rev. Lett.* **83**, 3398 (1999).
18. J. M. McGuirk, D. M. Harber, J. M. Obrecht, E. A. Cornell, *Phys. Rev. A* **69**, 062905 (2004).